DOI: 10.1002/ejic.200601004

Synthesis, Structure, and Reactivity of Cerium(IV) Calix[4]arene Complexes

Jochen Gottfriedsen,*[a] Reimo Hagner,[a] Marlies Spoida,[a] and Yuri Suchorski[a]

Keywords: Cerium / Calixarenes / Photoelectron spectroscopy

The equimolar reaction of $Ce(hfac)_4$ (**1**) (hfac = 1,1,1,5,5,5-hexafluoropentanedionato) with *p*-*t*Bu-calix[4](OMe)$_2$(OH)$_2$ in toluene gave the new cerium(IV) calix[4]arene complex {*p*-*t*Bu-calix[4](OMe)$_2$(O)$_2$}Ce(hfac)$_2$ (**2**). The single-crystal X-ray structure shows the cone geometry of the calixarene ligand with the methoxy groups coordinated to the cerium; it shows slightly longer cerium–oxygen (acetylacetonate ligand) bond lengths than the corresponding bonds in the analogous nonfluorinated complex {*p*-*t*Bu-calix[4](OMe)$_2$(O)$_2$}Ce(acac)$_2$ (**3**). The bromination reaction of **3** gave the bisbrominated complex {*p*-*t*Bu-calix[4](OMe)$_2$(O)$_2$}Ce(Br-acac)$_2$ (**4**). ^{1}H NMR spectroscopic studies and a single-crystal X-ray structure of **4** revealed that the bromination took place in the 3-position of the acac ligand. Furthermore, the first X-ray photoelectron spectroscopy (XPS) evaluation of the Ce oxidation state in cerium calix[4]arene complexes **2** and **3** is presented, and X-ray induced changes of Ce_{ox} in these complexes are detected.

Introduction

The coordination chemistry of cerium in the oxidation state +4 is dominated by its alkoxy and β-diketonate complexes. β-Diketonate complexes of cerium(IV) are well established as precursors in MOCVD (metal organic chemical vapor deposition) or ALE (atomic layer epitaxy) processes. The deposition of CeO_2 films as buffer layers for YBCO high temperature super conductor devices[1] were studied, and doped $Ce_{1-x}M_xO_{2-y}$ (M = Sm, Y, Gd) materials, which exhibit high oxygen ion conductivity, have been presented. These compounds are considered to be promising materials for solid oxide fuel cells, oxygen pumps, and methane conversion reactors.[2] Furthermore, the application of $Ce(tmhd)_4$ (tmhdH = 2,2,6,6-tetramethyl-3,5-heptanedione) as a dopant in SrS and $CaGa_2S_4$ thin films has been examined owing to the fact that cerium doping in these materials can produce blue–green and blue electroluminescent (EL) phosphors.[3] In addition to the studies on $Ce(tmhd)_4$,[1b,4] the suitabilities of the following other volatile β-diketonate complexes were investigated: $Ce(fdh)_4$ (fdhH = 6,6,6-trifluoro-2,2-dimethyl-3,5-hexanedione),[5] $Ce(fod)_4$ (fodH = 1,1,1,2,2,3,3-heptafluoro-7,7-dimethyloctane-4,6-dione),[6] $Ce(tmod)_4$ (tmodH = 2,2,7-trimethyl-3,5-octanedione),[7] and $Ce(txhd)_4$ (txhdH = 2,2,6-trimethyl-3,6-heptanedione).[7]

The high synthetic potential of Ce^{IV} β-diketonate complexes remains largely unexplored. Recently, literature reports indicated the synthesis of double-decker tetrapyrrole cerium complexes starting from $Ce(acac)_3(H_2O)_n$,[8] and our group reported the synthesis of {*p*-*t*Bu-calix[4](OMe)$_2$(O)$_2$}Ce(acac)$_2$ (**3**) from $Ce(acac)_4$.[9] A variety of methods have been used to study the valency of Ce in cerium complexes. Theoretical calculations[10] and XANES (X-ray absorption near-edge spectroscopy)[11] experiments, as well as studies of their magnetic properties,[11b] have been used to study the oxidation states of cerium COT (COT = cyclooctatetraenyl) and substituted COT complexes in detail,[12] which led to the conclusion that cerium is trivalent in these complexes. XANES studies of a series of double-decker tetrapyrrole cerium complexes[8a] also suggest partial delocalization of the ligand π electrons into a cerium 4f orbital, which results in a valency of 3.59 to 3.68. The XPS data of [Ce(Pc)$_2$] (Pc = phthalocyaninate) complexes revealed a valency that is neither tri- nor tetravalent, but a mixed valent state of them.[13] Calix[4]arene ligand systems are widely used to form complexes with almost all metal ions.[14] Complexes with cerium are still rare and mainly focused on Ce^{III} {e.g. cerium(III) calix[4]arene complexes [Ce(LH$_{-2}$)(MeOH)$_2$A]HA (L = 5,11,17,23-tetra-*tert*-butyl-25,27-bis(diethylcarbamoylmethoxy)-26,28-dihydroxycalix[4]arene, HA = picric acid)[15] and Ce(H$_2$O)$_5$(*p*-sulfonatocalix[4]arene + H$^+$)}.[16] Studies of the coordination behavior of *p*-*tert*-butylcalix[*n*]arene (*n* = 4–6) with tetravalent cerium in solution have also been performed.[17]

Here we present the synthesis of novel calix[4]arene complexes of Ce^{IV} using two different synthetic approaches. In addition to the synthesis starting from a homoleptic cerium β-diketonato complex, the reaction of {*p*-*t*Bu-calix[4](OMe)$_2$(O)$_2$Ce(acac)$_2$} (**3**) with Br_2 will be described to demonstrate its high synthetic potential in this class of cerium

[a] Chemisches Institut der Otto-von-Guericke, Universität Magdeburg,
Universitätsplatz 2, 39106 Magdeburg, Germany
Fax: +49-391-67-12933
E-mail: jochen.gottfriedsen@vst.uni-magdeburg.de

complexes. In addition to the standard characterization methods, NMR spectroscopy, MS, and single-crystal X-ray determination studies, we performed XPS experiments for two of the cerium calix[4]arene complexes to obtain the effective oxidation state of Ce in these complexes.

Results and Discussion

The equimolar reaction of $Ce(hfac)_4$ (**1**) (hfac = 1,1,1,5,5,5-hexafluoropentanedionato) with *p*-*t*Bu-calix[4](OMe)$_2$(OH)$_2$ in boiling toluene gave an immediate color change upon reaching the boiling point. After workup, the new cerium(IV) calix[4]arene complex {*p*-*t*Bu-calix[4](OMe)$_2$(O)$_2$}Ce(hfac)$_2$ (**2**) could be isolated as blue crystalline blocks (Scheme 1). Complex **2** is highly soluble in nonpolar organic solvents such as hexane, pentane, and toluene as well as in the polar solvents diethyl ether, THF, dichloromethane, and chloroform.

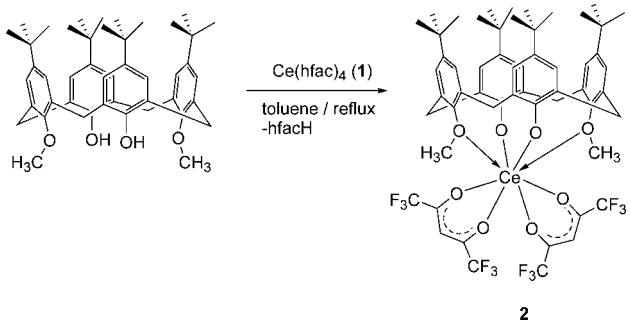

Scheme 1. Synthesis of **2**.

The reaction of the corresponding nonfluorinated Ce calix[4]arene complex {*p*-*t*Bu-calix[4](OMe)$_2$(O)$_2$}Ce(acac)$_2$ (**3**) with bromine in a 1:2 ratio in diethyl ether resulted in bromination of the acac ligand in the 3-position with formation of the bisbrominated complex {*p*-*t*Bu-calix[4](OMe)$_2$(O)$_2$}Ce(Br-acac)$_2$ (**4**) (Br-acac = 3-bromo-pentanedionato) (Scheme 2).

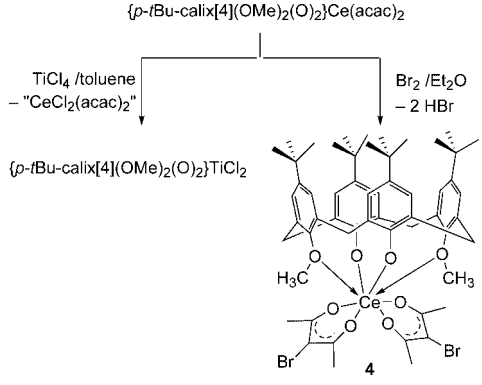

Scheme 2. Reactivity of **3** towards Br_2 and $TiCl_4$.

The reaction of **3** with bromine in a 1:1 ratio produced a monobrominated species which was detected by ^{1}H NMR spectroscopy but not isolated or further studied. Complex **4** exhibits the same solubility as that of **2** and the same blue color. The bromination of $Ce(acac)_4$ was described previously[18] by using NBS (*N*-bromosuccinimide) to yield $Ce(Br\text{-}acac)_4$. A ligand transfer to $TiCl_4$ was investigated to further elucidate the reactivity of complex **3**. Red crystals were obtained after crystallization from toluene, which where characterized by NMR spectroscopy and shown to be the known titanium complex {*p*-*t*Bu-calix[4](OMe)$_2$(O)$_2$}$TiCl_2$.[19] ^{1}H and ^{13}C NMR spectroscopic studies revealed the typical cone geometry of the calix[4]arene ligands for both complexes **2** and **4** in benzene solution. The ^{1}H NMR (Table 1) spectroscopic data show that the chemical shifts of the calix[4]arene ligand of brominated complex **4** are basically identical with those of starting material **3**, whereas the chemical shifts of **2** are significantly different, which is due to the electron-withdrawing fluorine substituents. The resonances of the methoxy group of complexes **2**, **3**, and **4** show the highest change in their chemical shifts compared with the corresponding ones of the free calix[4]arene ligand. Resonances of the methoxy group in all three complexes are shifted downfield by nearly 1.5 ppm for **2**, 1.25 ppm for **3**, and approximately 1 ppm for **4** relative to the chemical shift of the free ligand (δ =3.47 ppm). This is due to the electron-withdrawing fluorine atoms that induce a decrease in the electron density on the cerium atom, which is compensated by the coordinated methoxy group thus deshielding the CH_3 group. Doublets at 5.11 and 3.27 ppm for **2** and 5.04 and 3.35 ppm for **4** in the ^{1}H NMR spectra are attributable to the *endo* and *exo* protons of the CH_2 bridges of the calix[4]arene ligand. Whereas the chemical shifts of the *endo* protons are shifted downfield (nearly 0.7 ppm for **2** and 0.6 ppm for **4**) relative to the free calix[4]arene ligand, the resonances for the *exo* protons are not influenced by coordination to the cerium center. Two sets of signals for the aromatic hydrogens and the substituted tertiary butyl groups were found for each new complex, **2** and **4**, by assigning the two different ring systems of the calix[4]arene ligands (Table 1). The ^{13}C NMR spectra also show the two unequally substituted phenyl groups of the calixarene ligand in **2** and **4**. The different coordinationenvironments that are adopted by **1** (–76.51 ppm), **2** (–75.93 ppm), and 1,1,1,5,5,5-hexafluoropentanedione (–77.40 ppm) are made apparent in their ^{19}F NMR spectra,

Table 1. ^{1}H NMR spectroscopic data of complexes **2**, **3**, and **4** in C_6D_6 at 25 °C (δ in ppm).

	2	**3**	**4**
(s, 4 H, Ar*H*)	7.11	7.23	7.22
(s, 4 H, Ar*H*)	6.85	6.97	6.96
(d, *endo*-C*H*$_2$)	5.11	5.04	5.04
(d, *exo*-C*H*$_2$)	3.27	3.35	3.35
(s, 6 H, OC*H*$_3$)	4.93	4.72	4.58
(s, 18 H, CC*H*$_3$)	1.27	1.39	1.34
(s, 18 H, CC*H*$_3$)	0.90	0.98	0.97
(s, 2 H, COC*H*)	5.8	4.96	no signal
(s, 12 H, COC*H*$_3$)	no signal	1.76	2.19

which shows a small influence of the CF_3 groups on the chemical shift for this β-diketone. Mass spectrometric data of complexes **2** and **4** show the molecular ions as the signals with the highest mass. The signals with the highest abundance can be interpreted as the molecular ions reduced by the mass of the corresponding β-diketonate.

X-ray Structure Determinations

A single-crystal X-ray structure determination of the starting material $Ce(hfac)_4$ (**1**), which crystallized from toluene as dark brown crystals, was carried out. The molecular structure exhibits an eight-coordinate cerium in a distorted square antiprismatic coordination sphere (Figure 1).

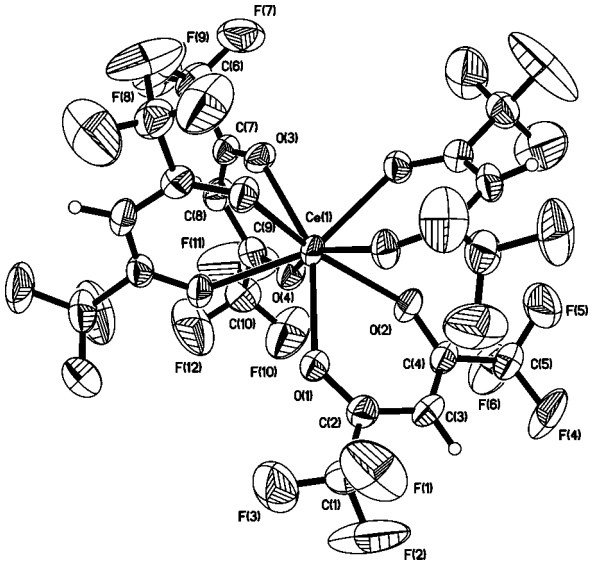

Figure 1. ORTEP plot of the molecular structure of **1**. Thermal ellipsoids are drawn with 50% probability. Hydrogen atoms are omitted for clarity.

The Ce–O bond lengths of the O,O′-bidentate hexafluoropentanedionato ligands range from 2.325(3) to 2.346(3) Å, which is in good agreement with similar distances found for cerium acetylacetonato complexes {e.g. α-$Ce(acac)_4$,[20a,20b] β-$Ce(acac)_4$,[20c] and $[Ce(acac)_4]\cdot 10H_2O$[21]}, which have a mean distance of 2.32 Å. Other cerium β-diketonato complexes display Ce–O distances between 2.24 Å and 2.36 Å [e.g. $Ce(fda)_4$, $Ce(tmhd)_4$, $Ce(txhd)_4$, and $Ce(tmod)_4$].

{*p*-*t*Bu-calix[4]$(OMe)_2(O)_2$}$Ce(hfac)_2$ (**2**) was crystallized from toluene at 5 °C and single crystals of the brominated complex {*p*-*t*Bu-calix[4]$(OMe)_2(O)_2$}$Ce(Br\text{-}acac)_2$ (**4**) were obtained from CH_2Cl_2 at 5 °C. The single-crystal X-ray structures of both complexes showed the typical cone geometry of the calixarene ligand with the methoxy groups coordinated to the cerium, which gave an eight coordinate cerium center with square antiprismatic coordination spheres (Figures 2 and 3).

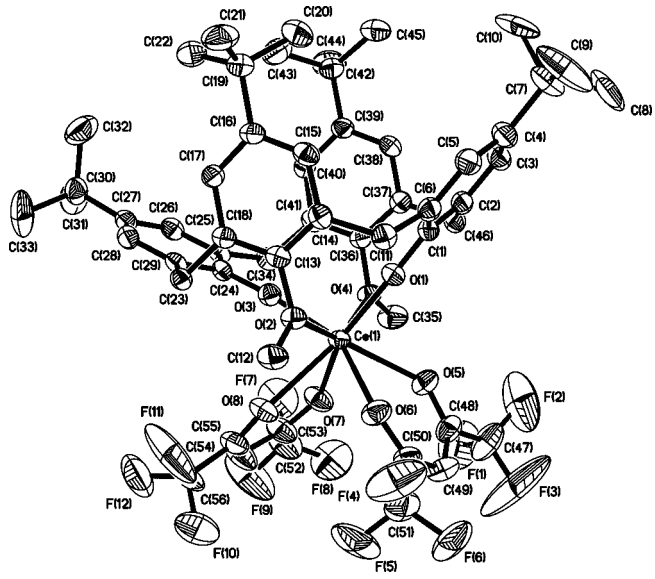

Figure 2. ORTEP plot of the molecular structure of **2**. Thermal ellipsoids are drawn with 50% probability. Hydrogen atoms are omitted for clarity.

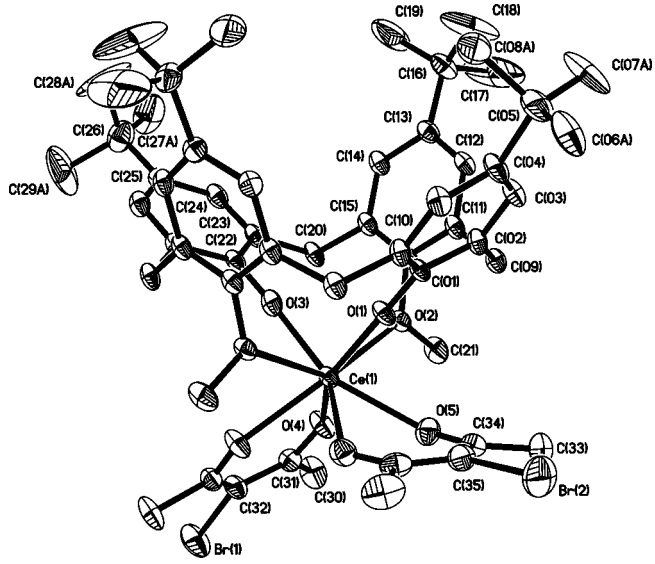

Figure 3. ORTEP plot of the molecular structure of **4**. Thermal ellipsoids are drawn with 50% probability. Hydrogen atoms are omitted for clarity.

The Ce–O phenoxy bond lengths in **2** [2.069(3)/2.089(3) Å] are slightly shorter than the corresponding distances in **4** [2.111(4)/2.134(5) Å], which are equal to the ones found for {*p*-*t*Bu-calix[4]$(OMe)_2(O)_2$}$Ce(acac)_2$ (**3**) (2.130 Å average)[9] (Table 2). They are in the same range as those in other cerium alkoxides {e.g. the hexafluoroisopropoxide (hfip) adducts $Ce(hfip)_4(TMEDA)$ and $Ce(hfip)_4$(diglyme) (2.13 Å average)M,[22] the terminal Ce–OR alkoxide groups in $Ce_2(O\text{i}Pr)_8(\text{i}PrOH)_2$ (2.088 Å average),[23] $Ce(O\text{t}Bu)_2(NO_3)_2(HO\text{t}Bu)_2$ (2.088 Å average),[24] and $Ce(O\text{t}Bu)_2(\mu\text{-}O\text{t}Bu)_2(\mu_3\text{-}O\text{t}Bu)_2Na_2(dme)_2$ [2.136–2.146 Å for the terminal (O*t*Bu) ligands]},[24] although they are longer than those observed for $Cp_3Ce^{IV}(O\text{t}Bu)$ (2.045 Å).[24] The

Table 2. Selected bond lengths [Å] and angles [°].

1		**2**		**4**	
Ce(1)–O(1)	2.346(3)	Ce(1)–O(3)	2.069(3)	Ce(1)–O(1)	2.111(4)
Ce(1)–O(2)	2.325(3)	Ce(1)–O(1)	2.089(3)	Ce(1)–O(3)	2.134(5)
Ce(1)–O(3)	2.334(3)	Ce(1)–O(7)	2.408(3)	Ce(1)–O(4)	2.365(3)
Ce(1)–O(4)	2.339(3)	Ce(1)–O(6)	2.409(4)	Ce(1)–O(4)[a]	2.365(3)
		Ce(1)–O(5)	2.426(3)	Ce(1)–O(5)	2.372(3)
		Ce(1)–O(8)	2.461(3)	Ce(1)–O(5)[a]	2.372(3)
		Ce(1)–O(4)	2.560(3)	Ce(1)–O(2)[a]	2.581(3)
		Ce(1)–O(2)	2.577(3)	Ce(1)–O(2)	2.581(3)
O(1)–Ce(1)–O(1)[a]	132.52(14)	O(3)–Ce(1)–O(1)	102.07(12)	O(1)–Ce(1)–O(3)	94.11(16)
O(2)–Ce(1)–O(1)	70.98(11)	O(3)–Ce(1)–O(7)	85.38(13)	O(1)–Ce(1)–O(4)	145.84(7)
O(2)–Ce(1)–O(3)	126.42(11)	O(1)–Ce(1)–O(7)	146.66(11)	O(3)–Ce(1)–O(4)	87.30(13)
O(2)–Ce(1)–O(4)	74.44(10)	O(3)–Ce(1)–O(6)	144.93(11)	O(1)–Ce(1)–O(4)[a]	145.84(7)
O(2)–Ce(1)–O(3)[a]	126.23(11)	O(1)–Ce(1)–O(6)	93.22(13)	O(3)–Ce(1)–O(4)[a]	87.30(13)
O(2)–Ce(1)–O(4)[a]	153.33(11)	O(7)–Ce(1)–O(6)	98.95(13)	O(4)–Ce(1)–O(4)[a]	68.31(15)
O(2)–Ce(1)–O(1)[a]	72.80(11)	O(3)–Ce(1)–O(5)	143.00(12)	O(1)–Ce(1)–O(5)	82.72(13)
O(2)[a]–Ce(1)–O(2)	78.92(16)	O(1)–Ce(1)–O(5)	85.51(11)	O(3)–Ce(1)–O(5)	145.17(8)
O(2)[a]–Ce(1)–O(3)	126.23(11)	O(7)–Ce(1)–O(5)	70.52(12)	O(4)–Ce(1)–O(5)	77.09(12)
O(3)–Ce(1)–O(1)	153.61(11)	O(6)–Ce(1)–O(5)	68.77(12)	O(4)[a]–Ce(1)–O(5)	114.41(11)
O(3)–Ce(1)–O(1)[a]	73.86(10)	O(3)–Ce(1)–O(8)	80.58(12)	O(1)–Ce(1)–O(5)[a]	82.72(13)
O(3)–Ce(1)–O(3)[a]	79.77(15)	O(1)–Ce(1)–O(8)	144.67(12)	O(3)–Ce(1)–O(5)[a]	145.17(8)
O(3)[a]–Ce(1)–O(1)	73.86(10)	O(7)–Ce(1)–O(8)	68.32(11)	O(4)–Ce(1)–O(5)[a]	114.41(11)
O(3)–Ce(1)–O(4)	71.18(11)	O(6)–Ce(1)–O(8)	69.16(12)	O(4)[a]–Ce(1)–O(5)[a]	77.09(12)
O(3)[a]–Ce(1)–O(4)	72.61(11)	O(5)–Ce(1)–O(8)	113.72(11)	O(5)–Ce(1)–O(5)[a]	69.09(16)
O(4)–Ce(1)–O(1)	99.27(11)	O(3)–Ce(1)–O(4)	76.17(10)	O(1)–Ce(1)–O(2)[a]	76.98(7)
O(4)–Ce(1)–O(1)[a]	99.50(11)	O(1)–Ce(1)–O(4)	79.56(11)	O(3)–Ce(1)–O(2)[a]	75.80(7)
O(4)–Ce(1)–O(4)[a]	132.22(15)	O(7)–Ce(1)–O(4)	70.67(11)	O(4)–Ce(1)–O(2)[a]	135.76(10)
		O(6)–Ce(1)–O(4)	138.20(10)	O(4)[a]–Ce(1)–O(2)[a]	70.29(9)
		O(5)–Ce(1)–O(4)	69.63(11)	O(5)–Ce(1)–O(2)[a]	135.80(10)
		O(8)–Ce(1)–O(4)	133.98(11)	O(5)[a]–Ce(1)–O(2)[a]	69.68(10)
		O(3)–Ce(1)–O(2)	81.08(11)	O(1)–Ce(1)–O(2)	76.98(7)
		O(1)–Ce(1)–O(2)	77.15(10)	O(3)–Ce(1)–O(2)	75.80(7)
		O(7)–Ce(1)–O(2)	136.15(10)	O(4)–Ce(1)–O(2)	70.29(9)
		O(6)–Ce(1)–O(2)	71.74(10)	O(4)[a]–Ce(1)–O(2)	135.76(10)
		O(5)–Ce(1)–O(2)	135.59(11)	O(5)–Ce(1)–O(2)	69.68(10)
		O(8)–Ce(1)–O(2)	68.40(10)	O(5)[a]–Ce(1)–O(2)	135.80(10)
		O(4)–Ce(1)–O(2)	143.03(9)	O(2)[a]–Ce(1)–O(2)	139.56(11)

[a] Atoms that are generated by using the symmetry transformation $-x + 1, y, -z + 1$ (**1**), and $x, -y, z$ (**4**), respectively.

Ce–O bond lengths for the two coordinated methoxy groups Ce(1)–O(2) and Ce(1)–O(4) in **2** [2.560(3)/2.577(3) Å] and Ce(1)–O(2) and Ce(1)–O(2)# in **4** [2.581(3) Å] are in the typical range of Ce–O coordination bonds[22] and fit well with the corresponding bonds in {*p*-*t*Bu-calix[4](OMe)$_2$(O)$_2$}Ce(acac)$_2$ (**3**) (2.604 Å average).[9] The Ce–O distances of the O,O′-bidentate hexafluoropentanedionato ligands in **2** range from 2.408(3) to 2.461(3) Å and are thus slightly longer than the distances found for starting material **1** [2.325(3) to 2.346(3) Å] and the Ce–O bonds of the two O,O′-bidentate acetylacetonate ligands in the analogous nonfluorinated complex {*p*-*t*Bu-calix[4](OMe)$_2$(O)$_2$}Ce(acac)$_2$ (**3**) (2.338 to 2.371 Å).[9] The corresponding Ce–O distances of the O,O′-bidentate 3-bromo-2,4-pentanedionato ligands to cerium in **4** [2.365(3) and 2.372(3) Å] match well with the ones of complex **3**. The Ce–O (β-diketonato) lengths of complexes **2** and **4** are only slightly longer than the Ce–O lengths found for the homoleptic cerium β-diketonate complexes. However, they are in good agreement with these lengths {e.g. α-Ce(acac)$_4$,[20a,20b] β-Ce(acac)$_4$,[20c] and [Ce(acac)$_4$](H$_2$O)$_{10}$,[21] with a mean distance of 2.32 Å, as well as Ce(fda)$_4$, Ce(tmhd)$_4$, Ce(txhd)$_4$, and Ce(tmod)$_4$, which exhibit Ce–O distances between 2.24 Å and 2.36 Å}.

The four donor atoms of the calixarene in **2**, **3**, and **4** define a mean O$_4$ plane with a rms deviation of 0.2464 Å in **2**, 0.2549 Å in **3**, and 0.2774 Å in **4** and the cerium atom is located at 1.0607(14) Å from this mean plane in **2**, 1.1641(10) Å in **3**, and 1.1686(20) Å in **4**. The macrocycles in new complexes **2** and **4**, as well as in **3**,[9] are in a distorted cone conformation, with dihedral angles between the four aromatic rings and the O$_4$ plane of 39.50(16), 89.50(11), 34.66(8), and 83.31(11)° in **2** [46.16(24), 71.72(9), 37.45(13), and 72.02(11)° in **4**]. The dihedral angles of the cone in **2** are similar to the ones in **3** [38.09(7), 83.86(7), 36.90(13), and 84.02(7)°], and to those found in [UCl$_2$(Me$_2$-calix)(THF)$_2$], [UCl$_2$(Me$_2$calix)(py)$_2$], and [U(acac)$_2$(Me$_2$calix)(THF)$_2$].[25] The slightly different values of the homologous angles in **4** might be due to crystal packing effects.

XPS Studies

High-resolution XPS spectra of complexes **2** and **3** were obtained by using monochromatic X-ray excitation. From

this spectra we determined the effective oxidation state of Ce (in the sense of an effective charge state of the Ce atoms in the ground state of the solid), Ce_{ox}. The Ce_{ox} value does not necessary represent the integral "formal valence" of Ce (in compounds with largely covalent character the formal valence does not approximate the actual ionic charge), but it reflects objectively the electronic structure of the studied materials. The direct use of established techniques, such as the commonly used deconvolution of high-resolution XPS spectra to evaluate the Ce_{ox} in coordination complexes, is still difficult despite a great effort devoted to the electronic structure of ceria and similar compounds. The main uncertainties are associated with the complex features in the Ce3d XPS-spectra and result from the variable occupancy of the Ce4f level, redistribution of the levels as a result of the core hole creation, and changed hybridization at different oxidation states.[26] Therefore, the interpretation of the spectra is not always unambiguous and can even be contradictory. In addition, artifacts created merely by the X-ray exposure have to be considered.[27] In the present work we evaluated Ce_{ox} in **2** and **3** by correlation of the XPS data for the studied samples with those of reference samples with a known oxidation state.

Ar-sputtered CeO_2 was used as the reference sample where the preferential release of oxygen atoms in the surface region, as a result of the impact of Ar^+ ions in ultrahigh vacuum (UHV), allows the creation of Ce_xO_y oxides in the top surface layers with continuously variable artificial Ce_{ox} in the range from 4 to 3.4. The details of the Ce_{ox} evaluation are published elsewhere.[28] A similar method was recently applied by us for the determination of the oxidation state of vanadium in vanadium oxide and vanadium/phosphate oxide catalysts.[29] The measurements of samples of both the studied complexes revealed an X-ray induced "photoreduction", an effect in principle known (but not entirely understood) for some rare earth containing materials such as, for example, Sm^{3+}-doped fluoroaluminate glasses[30] or for the pure CeO_2.[31] Thorough long-time studies of the X-ray-induced evolution of the Ce_{ox} revealed its exponential decay with increasing irradiation time (from 3.60 to 3.28 for **2** and from 3.62 to 3.27 for **3**) (Figure 4), where the extrapolation to "zero irradiation" (zero exposure) allows the determination of the initial oxidation state in the freshly synthesized complexes (3.61 for **2** and 3.65 for **3**). It has to be noted that in contrast to vanadium-containing oxide compounds, no UHV-induced modification of the cerium oxidation state was observed in the present study, that is, the observed effect is a pure X-ray-induced "photoreduction". The X-ray modified Ce_{ox} of cerium remained also stable after exposure to air at room temperature. Concerning the interpretation of the observed "photoreduction", we noted that the local irradiation-induced heating, proposed as a reduction mechanism for ceria,[31] cannot explain our observation as no significant increase in the surface temperature was observed. Apparently, alternative mechanisms such as the electron-hole pair formation and Auger decay have to be taken into account.[32] Another possible mechanism, associated with an impact of the numerous low-energy electrons,[33] which could cause desorption due to their large cross-section seems to be less probable, as was proven by low-energy electron bombardment from an external electron gun. Furthermore, a possible reason for the decrease in Ce_{ox} might be due to decomposition processes that are induced by the X-ray radiation, which leads to the formation of a mixture of cerium centers in the oxidation state 3 and 4. It should also be noted that the attenuation length of the Al K_α photons exceeds the XPS information depth of ≈ 2.5 nm, by at least three orders of magnitude, in the present case. Therefore, the irradiation-caused changes in the Ce oxidation state may extend to a significant depth.

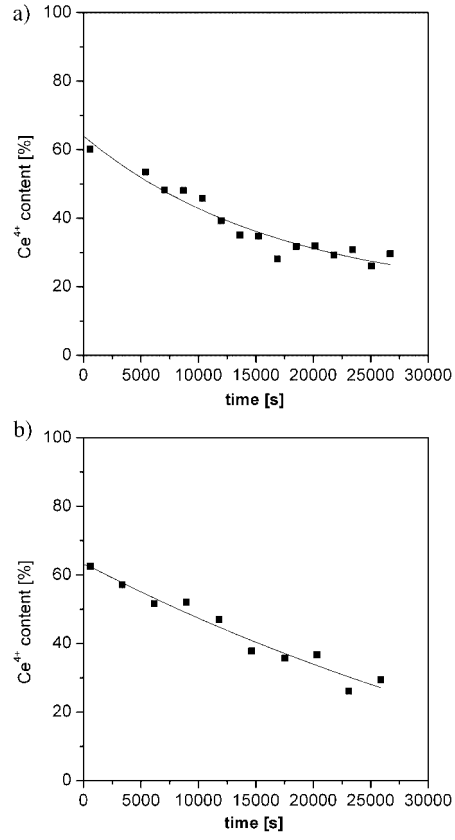

Figure 4. Dependencies of the Ce^{4+} content for **2** and **3**, respectively, on the X-ray exposure. Extrapolation to "zero irradiation" provides the initial values of Ce_{ox}.

Conclusions

Two novel cerium calix[4]arene complexes could be synthesized by using two different synthetic approaches. {*p*-*t*Bu-calix[4](OMe)$_2$(O)$_2$}Ce(hfac)$_2$ (**2**) was generated starting from a homoleptic cerium β-diketonato complex Ce(hfac)$_4$ (**1**). However, {*p*-*t*Bu-calix[4](OMe)$_2$(O)$_2$}Ce(Br-acac)$_2$ (**4**) was obtained from the reaction of {*p*-*t*Bu-calix[4](OMe)$_2$(O)$_2$}Ce(acac)$_2$ (**3**) with Br_2; thus, the high synthetic potential of this class of cerium complexes was demonstrated. Furthermore, we detected X-ray-induced changes in the effective Ce oxidation state in cerium calix-

[4]arene complexes **2** and **3**, and performed the first evaluation of Ce_{ox} in these complexes.

Experimental Section

General: All reactions were carried out under an inert atmosphere of dry nitrogen by using standard dry box and Schlenk techniques. Melting points were determined in a sealed capillary without correction. NMR spectra were recorded with a Bruker DPX 400 or AVANCE 600 NMR spectrometer. Chemical shifts (all reported in ppm) are referenced to tetramethylsilane as internal standard. Chemical shifts of the ^{13}C NMR were assigned to the corresponding carbons by using HSQC, HMBC, and NOSY techniques. In turn, chemical shifts of the ^{19}F NMR spectra are referenced to trifluorotoluene as external standard. The single-crystal X-ray diffraction studies were performed with a Bruker CCD SMART (**2**, **4**) or Stoe IPDS (**1**) diffractometer. Crystal data are given in Table 3. The structures were solved by Patterson methods (SHELXS-97).[34] Refinements were carried out by using full-matrix least-squares techniques on F^2 with the SHELXL-97 program.[35] CCDC-624482 (for **1**), -616674 (for **2**), and -624481 (for **4**) contain the supplementary crystallographic data for this paper. These data can be obtained free of charge from The Cambridge Crystallographic Data Centre via www.ccdc.cam.ac.uk/data_request/cif. Mass spectra (EI, 70 eV) were obtained with a Finnigan SSQ 7000 or a Finnigan MAT 95 (70 eV). Only characteristic fragments containing the isotopes of the highest abundance are listed. The starting materials *p*-*t*Bu-calix[4](OMe)$_2$(OH)$_2$[36] and {*p*-*t*Bu-calix[4](OMe)$_2$(O)$_2$}Ce(acac)$_2$[9] were produced according to a published procedure. Ce(hfac)$_4$ was synthesized by using a slightly modified procedure.[37] Elemental analyses were performed with a LECO CHNS932 apparatus. Hexafluoroacetylacetone and $(NH_4)_4[Ce(SO_4)_4]\cdot 2H_2O$ were purchased from Aldrich Chemical Co. and used as received. X-ray photoelectron spectra were obtained from the dry powders of **2** and **3**, which were carefully grinded and fixed on Mo sample-carrier plates under an argon atmosphere in a glove box and transferred inertly to the multipurpose UHV surface analysis apparatus (SPECS, Germany) where the XPS analyses were performed. To avoid the vacuum-induced reduction of the samples, a "fast transfer" XPS mode[29] was used: the SPECS load-lock and transfer systems allows sample-transfer times of less than 5 min between the start of the evacuation of the load lock and the first XPS spectrum at a pressure better than 5×10^{-9} mbar. The monochromatic X-ray source (FOCUS-500, SPECS, excitation energy 1253.74 eV, Al-K_α, linewidth after monochromatization $<$ 0.3 eV) was used. High-resolution spectra (pass energy 10 eV, step size 0.1–0.2 eV) were recorded at room temperature with a hemispherical energy analyzer (PHOIBOS-150, SPECS), which provides the possibility of simultaneous photo-electron detection on nine channels, and allows fast data acquisition times (0.5 s per data point) with a satisfactory signal-to-noise ratio.

Ce(hfac)$_4$ (1): $(NH_4)_4[Ce(SO_4)_4]\cdot 2H_2O$ (3.8 g, 6 mmol) in H_2O (200 mL) and 1,1,1,5,5,5-hexafluoro-2,4-pentanedione (5.0 g, 24 mmol) in toluene (100 mL) were mixed and stirred for 15 min, which resulted in a fast color change in the organic layer to dark brown. The two phases were separated, and toluene was removed under vacuum to leave a brown solid that was recrystallized from dry toluene (15 mL) to yield dark brown crystal blocks in 35% yield (2.03 g). ^1H NMR (400 MHz, C_6D_6, 25 °C): δ = 6.05 (s, 4 H, C*H*) ppm. ^{19}F NMR (376.5 MHz, C_6D_6, 25 °C): δ = –76.51 ppm. UV/Vis (250–800 nm, $CHCl_3$): λ = 275.6 nm.

{*p*-*t*Bu-calix[4](OMe)$_2$(O)$_2$}Ce(hfac)$_2$ (2): Ce(hfac)$_4$ (1.0 g, 1.03 mmol) and *p*-*t*Bu-calix[4](OMe)$_2$(OH)$_2$ (0.7 g, 1.03 mmol) were dissolved in toluene (50 mL), stirred at reflux temperature for 2 h, and another 12 h at room temperature. The reaction mixture was dried under vacuum (10^{-2} mbar) at 40 °C, and the resulting

Table 3. Crystal data and structural refinement for complexes **1**, **2**, and **4**.

	1	**2**	**4**
Empirical formula	$C_{20}H_4CeF_{24}O_8$	$C_{63}H_{68}CeF_{12}O_8$	$C_{60}H_{65}Br_2CeCl_4O_9$
Formula weight	968.35	1321.29	1371.86
Temperature [K]	180(2)	200(2)	180(2)
Wavelength [Å]	0.71073	0.71073	0.71073
Crystal system	monoclinic	triclinic	monoclinic
Space group	*I*2/*a*	$P\bar{1}$	*C*2/*m*
a [Å]	16.511(3)	13.3831(10)	28.049(6)
b [Å]	11.081(2)	14.3193(10)	15.198(3)
c [Å]	16.519(3)	16.9920(12)	16.611(3)
α [°]	90	102.0560(10)	90
β [°]	90.42(3)	98.3980(10)	118.84(3)
γ [°]	90	94.188(2)	90
Volume [Å^3]	3022.3(10)	3132.2(4)	6203(2)
Z, calcd. density [mg m^{-3}]	4, 2.128	2, 1.401	4, 1.469
Abs coeff [mm^{-1}]	1.698	0.814	2.246
F(000)	1848	1352	2772
Crystal size [mm]	$0.50\times0.50\times0.20$	$0.50\times0.40\times0.20$	$0.60\times0.50\times0.10$
θ range for data coll. [°]	2.47 to 27.96	2.01 to 29.29	3.54 to 27.96
Reflections collected	14035	21948	29279
Unique reflections	3583 (R_{int} = 0.0819)	12975 (R_{int} = 0.0268)	7645 (R_{int} = 0.0877)
Absorption correction	face indexed	SADABS	face indexed
Data/rest./parameters	3583/0/248	12975/0/928	7645/0/395
GOF on F^2	0.945	1.248	1.101
Final *R* indices [$I>2\sigma(I)$]	R_1 = 0.0445	R_1 = 0.0595	R_1 = 0.0576
	wR_2 = 0.1064	wR_2 = 0.1411	wR_2 = 0.1409
R indices (all data)	R_1 = 0.0572	R_1 = 0.0659	R_1 = 0.0716
	wR_2 = 0.1094	wR_2 = 0.1447	wR_2 = 0.1480

blue powder was dissolved in toluene (10 mL). Crystallization at 5 °C gave dark blue crystals in 79% yield (1.08 g, calculated as toluene solvate). M.p. 295 °C. ^{1}H NMR (400 MHz, C_6D_6, 25 °C): δ = 7.13 (m, 2 H, toluene), 7.11 (s, 4 H, Ar*H*), 7.05–7.0 (m, 3 H, toluene), 6.85 (s, 4 H, Ar*H*), 5.8 (s, 2 H, COC*H*), 5.11 [d, $^1J(^1H,^1H)$ = 12.6 Hz, *endo*-CH_2], 4.93 (s, 6 H, OCH_3), 3.27 [d, $^1J(^1H,^1H)$ = 12.6 Hz, *exo*-CH_2], 2.11 (s, 3 H, toluene), 1.27 (s, 18 H, CCH_3), 0.90 (s, 18 H, CCH_3) ppm. ^{13}C NMR (100.6 MHz, C_6D_6, 25 °C): δ = 177.57 (CF_3C-O), 173.57 [*C*(Ar)OCe], 152.54 [*C*(Ar)OCH$_3$], 148.53 (*t*Bu*C*), 145.92 (*t*Bu*C*), 133.45 (*C*CH$_2$), 133.4 (*C*CH$_2$), 129.30 (toluene), 128.31 (toluene), 126.29 [*C*H(Ar)], 125.66 (toluene), 122.19 [*C*H(Ar)], 118.5 (*C*F$_3$CO), 93.09 (CO*C*HCO), 67.96 (O*C*H$_3$), 34.02 (CH$_3$*C*), 33.48 (CH$_3$*C*), 32.46 (C*C*H$_3$), 31.31 (*C*H$_2$), 30.94 (C*C*H$_3$), 21.40 (toluene) ppm. ^{19}F NMR (376.5 MHz, C_6D_6, 25 °C): δ = –75.93 ppm. MS (EI, ^{140}Ce): *m*/*z* (%) = 1228 (5) $[M]^{+\cdot}$, 1021 (100) $[M - hfac]^+$, 1021 (40) $[M - hfac - CH_3]^+$. UV/Vis (250–800 nm, $CHCl_3$): λ = 276.8 nm. $C_{56}H_{60}CeF_{12}O_8C_7H_8$ (1321.31): calcd. C 57.27, H 5.19; found C 57.24, H 5.22.

{*p*-*t*Bu-calix[4](OMe)$_2$(O)$_2$}Ce(Br-acac)$_2$ (4): {*p*-*t*Bu-calix[4](OMe)$_2$(O)$_2$}Ce(acac)$_2$ (0.31 g, 0.31 mmol) was dissolved in diethyl ether (30 mL), and Br_2 (0.098 g, 0.62 mmol) was added by syringe at room temperature. The reaction mixture was heated under reflux for 3 h. The color of the solution changed from deep purple to deep blue. The solvent was removed under vacuum at 40 °C to give a blue powder, which was solved in dichloromethane (5 mL) and recrystallized at 5 °C to yield small cube-like crystals in 45% yield (0.16 g). M.p. 310 °C. ^{1}H NMR (400 MHz, C_6D_6, 25 °C): δ = 7.22 (s, 4 H, Ar*H*), 6.96 (s, 4 H, Ar*H*), 5.04 [d, $^1J(^1H,^1H)$ = 12.1 Hz, *endo*-CH_2], 4.58 (s, 6 H, OCH_3), 3.35 [d, $^1J(^1H,^1H)$ = 12.1 Hz, *exo*-CH_2], 2.19 (s, 12 H, COCH_3), 1.34 (s, 18 H, CCH_3), 0.97 (s, 18 H, CCH_3) ppm. ^{13}C NMR (100.6 MHz, C_6D_6, 25 °C): δ = 187.72 (CH$_3$*C*-O), 170.57 [*C*(Ar)OCe], 153.71 [*C*(Ar)OCH$_3$], 147.56 (*t*Bu*C*), 141.39 (*t*Bu*C*), 133.17 (*C*CH$_2$), 132.39 (*C*CH$_2$), 125.94 (*C*H), 123.49 (*C*H), 100.66 (CO*C*BrCO), 66.79 (O*C*H$_3$), 34.01 (CH$_3$*C*), 33.82 (CH$_3$*C*), 32.43 (*C*H$_2$), 32.32 (C*C*H$_3$), 31.13 (C*C*H$_3$), 28.82 (*C*H$_3$CO) ppm. MS (EI, ^{140}Ce): *m*/*z* (%) = 1170 (5) $[M]^{+\cdot}$, 993 (100) $[M - (Br\text{-}acac)]^+$, 912 (60) $[M - (Br\text{-}acac) - Br]^+$. UV/Vis (250–800 nm, $CHCl_3$): λ = 289.8 nm. $C_{56}H_{70}Br_2CeO_8$ (1171.07): calcd. C 57.43, H 6.02; found C 57.23, H 6.04.

Synthesis of {*p*-*t*Bu-calix[4](OMe)$_2$(O)$_2$}TiCl$_2$ from {*p*-*t*Bu-calix[4](OMe)$_2$(O)$_2$}Ce(acac)$_2$ and TiCl$_4$: {*p*-*t*Bu-calix[4](OMe)$_2$(O)$_2$-Ce(acac)$_2$} (1.7 g, 1.7 mmol) was dissolved in toluene (50 mL) and $TiCl_4$ (0.096 g, 1.7 mmol) was added by syringe at room temperature, which caused the color of the solution to change to red. Subsequent stirring for another 12 h and removal of the solvent under vacuum gave a red–brown powder that was recrystallized from toluene (10 mL) to afford deep red crystals. ^{1}H NMR (400 MHz, C_6D_6, 25 °C): δ = 7.17 (s, 4 H, Ar*H*), 6.82 (s, 4 H, Ar*H*), 4.61 [d, $^1J(^1H,^1H)$ = 13.4 Hz, *endo*-CH_2], 4.18 (s, 6 H, OCH_3), 3.18 [d, $^1J(^1H,^1H)$ = 13.4 Hz, *exo*-CH_2], 1.38 (s, 18 H, CCH_3), 0.69 (s, 18 H, CCH_3) ppm.

Acknowledgments

The authors thank Dr. S. Blaurock for solving the X-ray structures, Prof. Krautscheid (University of Leipzig, Germany) for providing the single-crystal X-ray facilities, and Prof. Frank T. Edelmann for helpful discussions, as well, R. Wrobel and B. Strzelczyk are thanked for the performance of the XPS studies. This work was financially supported by the Otto-von-Guericke-University of Magdeburg.

[1] a) X. D. Wu, R. C. Dye, R. E. Muenchausen, S. R. Foltyn, M. Maley, A. D. Rollett, A. R. Garcia, N. S. Nogar, *Appl. Phys. Lett.* **1991**, *58*, 2165; b) Z. Lu, R. Hiskes, S. A. DiCarolis, A. Nel, R. K. Route, R. S. Feigelson, *J. Cryst. Growth* **1995**, *156*, 227.
[2] a) F. Eguchi, T. Setoguchi, T. Inoue, H. Arai, *Solid State Ionics* **1992**, *52*, 165; b) D. L. Maricle, T. E. Swarr, S. Karavolis, *Solid State Ionics* **1992**, *52*, 173.
[3] a) P. Soininen, L. Niinistö, E. Nykänen, M. Leskelä, *Appl. Surf. Sci.* **1994**, *75*, 99; b) D. Endisch, K. Barth, J. Lau, G. Peterson, A. E. Kaloyeros, D. Tuenge, C. N. King, *Mater. Res. Soc. Symp. Proc.* **1997**, *471*, 269; c) J. E. Lau, K. W. Barth, G. G. Peterson, D. Endisch, A. Topol, A. E. Kaloyeros, R. T. Tuenge, M. J. DelaRosa, C. N. King, *J. Electrochem. Soc.* **1998**, *145*, 4271; d) T. S. Moss, R. C. Dey, D. C. Smith, J. A. Samuels, M. J. DelaRosa, C. F. Schaus, *Mater. Res. Soc. Symp. Proc.* **1996**, *415*, 21; e) T. S. Moss, R. C. Dey, M. J. DelaRosa, C. F. Schaus, *Proc. Electrochem. Soc.* **1996**, *96–5*, 396.
[4] a) H. Song, Y. Jiang, C. Xia, G. Meng, D. Peng, *J. Cryst. Growth* **2003**, *250*, 423–430; b) M. Pan, H. W. Meng, C. S. Chen, D. K. Peng, Y. S. Lin, *Thin Solid Films* **1998**, *324*, 89; c) H. Z. Song, H. B. Wang, J. Zhang, D. K. Peng, G. Y. Meng, *Mater. Res. Bull.* **2002**, *37*, 1487.
[5] a) M. Becht, K.-H. Dahmen, V. Gramlich, A. Marteletti, *Inorg. Chim. Acta* **1996**, *248*, 27; b) M. Becht, T. Gerfin, K.-H. Dahmen, *Chem. Mater.* **1993**, *5*, 137–144.
[6] J. McAleese, J. C. Plakatourras, B. C. H. Steele, *Thin Solid Films* **1996**, *280*, 152.
[7] M. J. DelaRosa, K. S. Bousman, J. T. Welch, P. J. Toscano, *J. Coord. Chem.* **2002**, *55*, 781.
[8] a) Y. Bian, J. Jiang, Y. Tao, M. T. M. Choi, R. Li, A. C. H. Ng, P. Zhu, N. Pan, X. Sun, D. P. Arnold, Z.-Y. Zhou, H.-W. Li, T. C. W. Mak, D. K. P. Ng, *J. Am. Chem. Soc.* **2003**, *125*, 12257; b) J. Jiang, W. Liu, K.-W. Poon, D. Du, D. P. Arnold, D. K. P. Ng, *Eur. J. Inorg. Chem.* **2000**, 205.
[9] J. Gottfriedsen, D. Dorokhin, *Z. Anorg. Allg. Chem.* **2005**, *631*, 2928.
[10] M. Dolg, P. Fulde, H. Stoll, H. Preuss, A. Chang, R. M. Pitzer, *Chem. Phys.* **1995**, *195*, 71.
[11] a) N. M. Edelstein, P. G. Allen, J. J. Bucher, D. K. Shuh, C. D. Sofield, *J. Am. Chem. Soc.* **1996**, *118*, 13115; b) C. H. Booth, M. D. Walter, M. Daniel, W. W. Lukens, R. A. Andersen, *Phys. Rev. Lett.* **2005**, *95*, 267202.
[12] a) For a recent review of Ce^{IV} [8]annulene complexes, see: F. T. Edelmann, D. M. M. Freckmann, H. Schumann, *Chem. Rev.* **2002**, *102*, 1851; b) A. Streitwieser, S. A. Kinsley, C. H. Jenson, J. T. Rigsbee, *Organometallics* **2004**, *23*, 5169; c) H.-D. Amberger, H. Reddmann, F. T. Edelmann, *J. Organomet. Chem.* **2005**, *690*, 2238.
[13] H. Isago, M. Shimoda, *Chem. Lett.* **1992**, 147.
[14] P. Thuéry, M. Nierlich, J. Harrowfield, M. Ogden, *Calixarenes 2001* (Eds.: Z. Asfari, V. Böhmer, J. Harrowfield, J. Vicens), Kluwer, Dordrecht, **2001**, ch. 30, p. 561 and references cited therein.
[15] P. D. Beer, M. G. B. Drew, A. Grieve, M. I. Ogden, *J. Chem. Soc., Dalton Trans.* **1995**, 3455.
[16] J. L. Atwood, L. J. Barbour, S. Dalgarno, C. L. Raston, H. R. Webb, *J. Chem. Soc., Dalton Trans.* **2002**, 4351.
[17] Z. Yawen, Y. Chunhua, M. Yoshitaka, *J. Rare Earths* **2002**, *20*, 41.
[18] G. Shankar, S. K. Ramalingam, *Transition Met. Chem.* **1984**, *9*, 449.
[19] a) U. Radius, A. Friedrich, *Z. Anorg. Allg. Chem.* **1999**, *625*, 2154; b) A. Zanotti-Gerosa, E. Solari, L. Giannini, C. Floriani, N. Re, A. Chiesi-Villa, C. Rizzoli, *Inorg. Chim. Acta* **1998**, *270*, 298.
[20] a) B. Matković, D. Grdenić, *Acta Crystallogr.* **1963**, *16*, 456; b) H. Titze, *Acta Chem. Scand. A* **1974**, *28*, 1079; c) H. Titze, *Acta Chem. Scand.* **1969**, *23*, 399.

[21] T. Behrsing, A. M. Bond, G. B. Deacon, C. M. Forsyth, M. Forsyth, K. J. Kamble, B. W. Skelton, A. H. White, *Inorg. Chim. Acta* **2003**, *352*, 229.
[22] S. Daniele, L. G. Hubert-Pfalzgraf, M. Perrin, *Polyhedron* **2002**, *21*, 1985.
[23] B. A. Vaartstra, J. C. Huffman, P. S. Gradeff, L. G. Hubert-Pfalzgraf, J. C. Daran, S. Parraud, K. Yunlu, K. G. Caulton, *Inorg. Chem.* **1990**, *29*, 3126.
[24] W. J. Evans, T. J. Deming, J. M. Olofson, J. W. Ziller, *Inorg. Chem.* **1989**, *28*, 4027.
[25] L. Salmon, P. Thuéry, Z. Asfari, M. Ephritikhine, *Dalton Trans.* **2006**, 3006–3014.
[26] a) A. Pfau, K. D. Schierbaum, *Surf. Sci.* **1994**, *321*, 71; b) E. Wuilloud, B. Delley, W.-D. Schneider, Y. Baer, *Phys. Rev. Lett.* **1984**, *53*, 202; c) D. R. Mullins, S. H. Overbury, D. R. Huntley, *Surf. Sci.* **1998**, *409*, 307.
[27] L. El Fallah, L. Hilaire, B. Romeo, F. Le Normand, *J. Electron. Spectrosc. Relat. Phenom.* **1995**, *73*, 89.
[28] Y. Suchorski, J. Gottfriedsen, R. Wrobel, B. Strzelczyk, H. Weiss, *Solid State Phenom.* **2007**, *128*, 115–122.
[29] Y. Suchorski, L. Rihko-Struckmann, F. Klose, Y. Ye, M. Alandjiyska, K. Sundmacher, H. Weiss, *Appl. Surf. Sci.* **2005**, *249*, 231.
[30] J. Qiu, K. Nouch, K. Miura, T. Mitsuyu, K. Hirao, *J. Phys.: Condens. Matter* **2000**, *12*, 5061.
[31] E. Paparazzo, G. M. Ingo, *J. Electron. Spectrosc. Relat. Phenom.* **1998**, *95*, 301.
[32] a) J. Cazaux, *J. Electron. Spectrosc. Relat. Phenom.* **1999**, *105*, 155; b) S. P. Chenakin, R. Prada Silvy, N. Kruse, *Catal. Lett.* **2005**, *102*, 39.
[33] a) R. G. Copperthwhite, J. Lloyd, *Nature* **1978**, *271*, 141; b) D. E. Ramaker, C. T. White, J. S. Murday, *J. Vac. Sci. Technol.* **1981**, *18*, 74.
[34] G. M. Sheldrick, *SHELXS-97, Program of Crystal Structure Solution*, University of Göttingen, Göttingen, Germany, **1997**.
[35] G. M. Sheldrick, *SHELXL-97, Program of Crystal Structure Refinement*; University of Göttingen: Göttingen, Germany, **1997**.
[36] A. Arduini, A. Casnati in *Macrocycle Synthesis* (Ed.: O. Parker), Oxford University Press, New York, **1996**, ch. 7.
[37] T. Yoshimura, C. Miyake, S. Imoto, *Bull. Chem. Soc. Jpn.* **1973**, *46*, 2096–2101.

Received: October 24, 2006
Published Online: April 17, 2007

